NREL
NATIONAL RENEWABLE ENERGY LABORATORY

An Analytical Approach Treating Three-Dimensional Geometrical Effects of Parabolic Trough Collectors

Preprint

Marco Binotti
National Renewable Energy Laboratory, visiting student from Politecnico di Milano

Guangdong Zhu and Allison Gray
National Renewable Energy Laboratory

Giampaolo Manzolini
Politecnico di Milano

To be presented at the 2012 World Renewable Energy Forum
Denver, Colorado
May 13–17, 2012

Conference Paper
NREL/CP-5500-54712
April 2012

Contract No. DE-AC36-08GO28308

Available electronically at http://www.osti.gov/bridge

Available for a processing fee to U.S. Department of Energy
and its contractors, in paper, from:

U.S. Department of Energy
Office of Scientific and Technical Information
P.O. Box 62
Oak Ridge, TN 37831-0062
phone: 865.576.8401
fax: 865.576.5728
email: mailto:reports@adonis.osti.gov

Available for sale to the public, in paper, from:

U.S. Department of Commerce
National Technical Information Service
5285 Port Royal Road
Springfield, VA 22161
phone: 800.553.6847
fax: 703.605.6900
email: orders@ntis.fedworld.gov
online ordering: http://www.ntis.gov/help/ordermethods.aspx

Cover Photos: (left to right) PIX 16416, PIX 17423, PIX 16560, PIX 17613, PIX 17436, PIX 17721

Printed on paper containing at least 50% wastepaper, including 10% post consumer waste.

AN ANALYTICAL APPROACH TREATING THREE-DIMENSIONAL GEOMETRICAL EFFECTS OF PARABOLIC TROUGH COLLECTORS

Marco Binotti
Visiting PhD student from Politecnico di Milano
National Renewable Energy Laboratory
Golden, CO, USA

Guangdong Zhu
National Renewable Energy Laboratory
Golden, CO, USA
Guangdong.Zhu@nrel.gov

Allison Gray
National Renewable Energy Laboratory
Golden, CO, USA

Giampaolo Manzolini
Politecnico di Milano
Milano, Italy

ABSTRACT

An analytical approach, as an extension of one newly developed method — **First**-principle **OPT**ical **I**ntercept **C**alculation (FirstOPTIC) — is proposed to treat the geometrical impact of three-dimensional (3-D) effects on parabolic trough optical performance. The mathematical steps of this analytical approach are presented and implemented numerically as part of the suite of FirstOPTIC code. In addition, the new code has been carefully validated against ray-tracing simulation results and available numerical solutions. This new analytical approach to treating 3-D effects will facilitate further understanding and analysis of the optical performance of trough collectors as a function of incidence angle.

1. INTRODUCTION

Recently, after a long period of lethargy, concentrating solar power (CSP) has experienced revived market growth, with an installed capacity of about 740 MW between 2007 and 2010. At the end of 2010, the global installed capacity accumulated to about 1,095 MW and is forecasted to reach about 1,789 MW [1] by the end of 2013. There are four main CSP technologies: parabolic trough, linear-Fresnel, central-receiver tower, and dish/engine. Parabolic trough, as the reference CSP technology, accounts for about 90% of existing commercial CSP plants. A key parameter for the evaluation of parabolic trough technology is the collector optical performance, which has an immediate impact on the levelized cost of energy (LCOE) of a solar plant. The nominal optical efficiency of a trough collector is calculated at normal incidence and defined as:

$$\eta_o = \frac{E_{receiver}}{E_{sun}} = \rho\tau\alpha\gamma. \quad (1)$$

Here, ρ is the parabolic mirror reflectivity, τ the receiver glass envelope transmissivity, α the average receiver coating absorptivity, and γ the collector intercept factor. The intercept factor accounts for the fraction of reflected rays that reach the receiver tube. The factors determining a collector's intercept factor include the finite size of the sun shape and various collector optical errors such as mirror specularity error, mirror slope error, receiver position error, and collector tracking error.

Parabolic trough collectors track the sun in the transversal plane, while in the longitudinal plane the incidence angle varies over time, leading to reduced optical performance. Here, the incidence angle of a trough collector is defined as the angle between the normal vector to the collector aperture plane and the nominal direction of incoming sun rays. The effects of varying incidence angle (θ) on parabolic trough collectors are often called *three-dimensional (3-D) effects*. These 3-D effects have been examined extensively in the past [2] and include the cosine effect, the widened image of the sun, the end loss, the elongated optical path of reflected rays, and the decaying material optical performance with increasing incidence angle.

The incidence angle modifier (IAM) is defined to account for the 3-D effects as follows:

$$IAM(\theta) = \frac{\eta(\theta)}{\eta_0(\theta = 0)}. \quad (2)$$

Here, the IAM includes the cosine effect. The work here focuses on the geometrical impact of 3-D effects, so the decaying material optical performance (such as decaying absorptivity of the receiver coating surface) is not included in the calculation of IAM. However, it must be mentioned that material performances are dependent on the incidence angle and may vary with different adopted technologies of trough collectors.

This paper discusses the development of an analytical methodology to correctly model the geometrical impacts of the incidence angle θ on the intercept factor. In Section 2, an overview of FirstOPTIC [3] is given. Section 3 presents a mathematical procedure treating the various 3-D effects as an extension of FirstOPTIC. The code development and validation are described in Section 4. Lastly, the conclusions are outlined in Section 5.

2. THE FirstOPTIC AT NORMAL INCIDENCE

FirstOPTIC calculates the intercept factor of a trough collector by employing first-principle treatment to optical error sources and was described in detail by Zhu & Lewandowski [3]. Here, a brief introduction is given.

For a trough collector, various optical error sources such as mirror specularity and tracking error effectively broaden the original sun shape, which results in an effective broadened beam cone reaching the receiver. Assume the effective broadened beam is represented by the following function:

$$B_{eff} = g_{eff}(\beta). \tag{3}$$

The effective beam spread function in the above equation may include the effect of all or part of the system optical errors. Assume the effective beam of equation (3) accounts for all system optical errors excluding reflector slope error and receive position error, which are instead represented as a geometrical error data set affecting the collector's acceptance angles.

For an arbitrary point (x,y) on a trough collector under normal incidence, the local intercept factor can be calculated as:

$$\gamma(x,y) = \int_{\beta^-_{slope+receiver(x,y)}}^{\beta^+_{slope+receiver}(x,y)} g_{eff}(\beta)\, d\beta. \tag{4}$$

Here, $\beta^+_{slope+receiver}(x,y)$ and $\beta^-_{slope+receiver}(x,y)$ are the receiver acceptance angle limits accounting for both mirror slope error and receiver position error. The impact of slope error and position error on the acceptance angles is illustrated in Fig. 1.

Integration of $\gamma(x,y)$over the trough aperture yields the intercept factor:

$$\gamma_0 = \frac{1}{w \cdot l} \cdot \int_{-\frac{l}{2}}^{-\frac{l}{2}} \int_{-\frac{w}{2}}^{\frac{w}{2}} \gamma(x,y) dx dy. \tag{5}$$

A suite of MATLAB code has been developed and validated for FirstOPTIC. In the FirstOPTIC code, the system optical errors can be defined either as probability distribution functions or in a format representing direct laboratory measurements for mirror slope errors and receiver position errors. Please refer to Zhu & Lewandowski [3] for details.

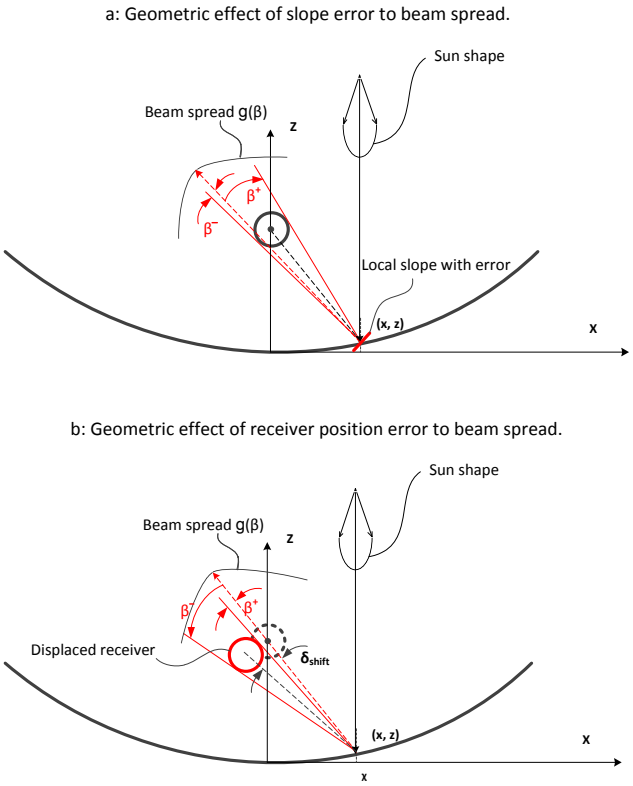

Fig. 1: Illustration of collector acceptance angles with slope error (top) and receiver position (bottom) error present.

3. MATHEMATICAL MODEL TREATING THE 3-D EFFECTS

The existing FirstOPTIC was developed for trough collectors under normal incidence. Under non-zero incidence angles, the acceptance angle limits β^+_{3D} and β^-_{3D} are not only a function of transversal slope errors and receiver position error, but also a function of the incidence angle and of the longitudinal slope errors. The rest of this section is focused on the development of generic mathematical formulae to calculate new acceptance angles for varying incidence angles. Once the acceptance angle limits are obtained, the intercept factor can then be readily calculated through equations (4) and (5).

3.1 Theoretical derivation of acceptance angle under non-zero incidence

I. Determination of the actual normal vector for every point of the mirror

Mirror slope errors in the first-principle approach are treated as rotations of the normal vector to the desired mirror surface. For mathematical convenience, two different coordinate systems are used: a global coordinate system (*x, y, z*) and a local coordinate system (x', y', z') centered in a selected surface point, in which the x' axis is tangent to the trough surface in the *xz* plane as shown in Fig. 2.

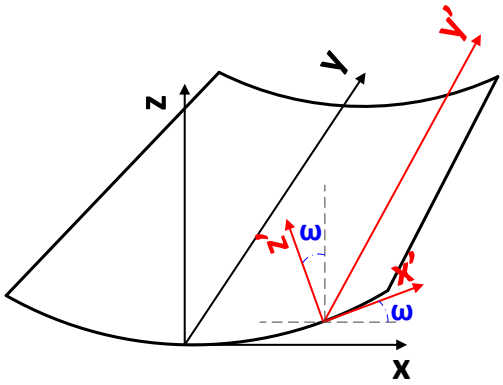

Fig. 2: Adopted reference axes systems.

For an arbitrary point $P(x_0, y_0, z_0)$ on the reflector surface, the normal unit vector to the surface is $n' = [0, 0, 1]$ in the local coordinate axis system and $n = [-sin(\omega), 0, cos(\omega)]$, with $\omega = \text{atan}\left(\frac{\partial z}{\partial x}\right) = \tan^{-1}\left(\frac{x}{2f}\right)$, in the global coordinate system. Usually slope errors are obtained through experimental measurements [4] as angular displacement in the longitudinal (ε_y) and transversal planes (ε_x) with respect to the local coordinate system. The slope error is defined as positive here if it causes a clockwise rotation of the normal vector. The actual surface normal vector n'_ε with slope errors present is:

$$\vec{n}'_\varepsilon = \begin{bmatrix} \frac{tan\varepsilon_x}{\sqrt{1+tan^2\varepsilon_y+tan^2\varepsilon_x}} \\ \frac{tan\varepsilon_y}{\sqrt{1+tan^2\varepsilon_y+tan^2\varepsilon_x}} \\ \frac{1}{\sqrt{1+tan^2\varepsilon_y+tan^2\varepsilon_x}} \end{bmatrix} \quad (6)$$

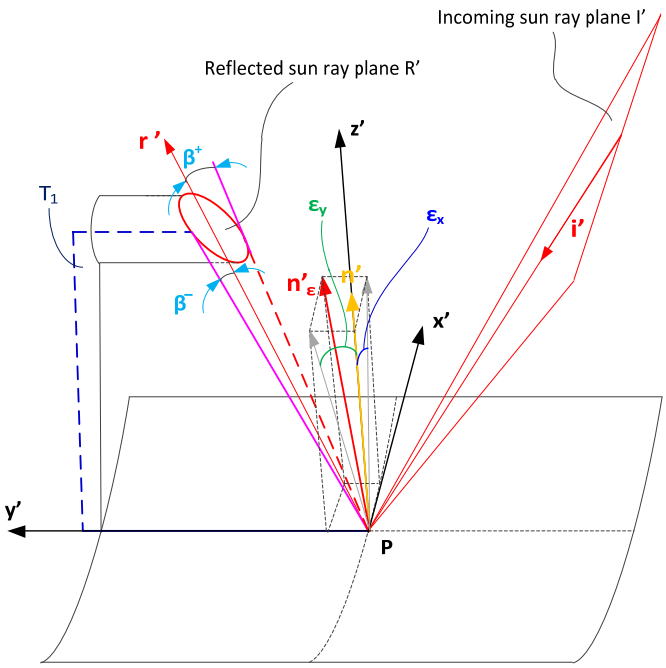

Fig. 3: Illustration of acceptance angle calculation for a trough collector.

II. Determination of the plane containing the incoming rays and reflected rays

As illustrated in Fig. 3, the incoming sun plane with an incidence angle θ is denoted by its nominal incoming vector i' and the incoming plane normal vector $i'_\perp$ as follows:

$$\vec{\imath}' = \begin{bmatrix} cos\theta sin\omega \\ sin\theta \\ cos\theta cos\omega \end{bmatrix};\ \vec{\imath}'_\perp = \begin{bmatrix} sin\theta sin\omega \\ -cos\theta \\ sin\theta cos\omega \end{bmatrix}. \quad (7\text{-}8)$$

Here, the incidence angle θ is the angle between the nominal incoming vector i' and the transversal plane $x'z'$.

With Snell's law, the nominal reflected ray r' and the unit vector $r'_\perp$ normal to the reflected plane R' containing the reflected rays can be obtained:

$$\vec{r}' = -\vec{\imath}' + 2(\vec{\imath}' \cdot \vec{n}'_\varepsilon) \cdot \vec{n}'_\varepsilon \quad (9)$$

$$\vec{r}'_\perp = -\vec{\imath}'_\perp + 2(\vec{\imath}'_\perp \cdot \vec{n}'_\varepsilon) \cdot \vec{n}'_\varepsilon \quad (10)$$

III. Determination of the planes passing through P and tangent to the absorber tube

Assuming the receiver position error $(\Delta x, \Delta z)$, the acceptance angle limits in the transversal plane ($x'z'$) can be calculated by FirstOPTIC as [3]:

$$\beta^{+}_{receiver}(x) = \delta_{shift}(x) + \sin^{-1}\left\{\frac{d}{2\cdot\sqrt{\left[(x-\Delta x)^2+\left(\frac{x^2}{4\cdot f}-f-\Delta z\right)^2\right]}}\right\}$$

$$\beta^{-}_{receiver}(x) = \delta_{shift}(x) - \sin^{-1}\left\{\frac{d}{2\cdot\sqrt{\left[(x-\Delta x)^2+\left(\frac{x^2}{4\cdot f}-f-\Delta z\right)^2\right]}}\right\} \quad (11\text{-}12)$$

Here, $\delta_{shift}(x)$ is the shifted angle for the center of the receiver due to position errors expressed in the vector's operation as:

$$\delta_{shift}(x) = \frac{(\overrightarrow{v_o} \times \overrightarrow{v_n})_y}{\left|(\overrightarrow{v_o} \times \overrightarrow{v_n})_y\right|} \cdot \cos^{-1}\left(\frac{\overrightarrow{v_o} \cdot \overrightarrow{v_n}}{|\overrightarrow{v_o}| \cdot |\overrightarrow{v_n}|}\right), \quad (13)$$

where

$$\vec{v}_o = \begin{pmatrix} x \\ 0 \\ z-f \end{pmatrix}; \quad \vec{v}_n = \begin{pmatrix} x-\Delta x \\ 0 \\ z-f-\Delta z \end{pmatrix}. \quad (14\text{-}15)$$

The plane T_1 and T_2 are tangent to the receiver surface. Then, the normal vectors to the planes T_1 and T_2 are:

$$\vec{n}_{\perp T1} = \begin{bmatrix} \cos(\omega+\beta^{+}_{receiver}) \\ 0 \\ \sin(\omega+\beta^{+}_{receiver}) \end{bmatrix}; \quad (16)$$

$$\vec{n}_{\perp T2} = \begin{bmatrix} \cos(\omega+\beta^{-}_{receiver}) \\ 0 \\ \sin(\omega+\beta^{-}_{receiver}) \end{bmatrix}. \quad (17)$$

Thus, the equations of the two planes are:

$$T_1: \cos(\omega+\beta^{+}_{receiver})\,x' + \sin(\omega+\beta^{+}_{receiver})z' = 0 \quad (18)$$

$$T_2: \cos(\omega+\beta^{-}_{receiver})\,x' + \sin(\omega+\beta^{-}_{receiver})\,z' = 0 \quad (19)$$

IV. Determination of the acceptance angles under non-zero incidence angle

The acceptance angles for point *P* are the angles between the vector *r'* and the two vectors L_1 and L_2, which are two intersections $R' \bigcap T_1$ and $R' \bigcap T_2$. To calculate the vector L_1, first:

$$L_1 = R' \bigcap T_1 = \begin{cases} n_{\perp T1}(1)x' + n_{\perp T1}(3)z' = 0; \\ r'_{\perp}(1)x' + r'_{\perp}(3)z' = -r'_{\perp}(2)y'. \end{cases} \quad (20)$$

The above system is solved to obtain the following solution of L_1:

$$\begin{cases} \overline{x_1} = \dfrac{\begin{vmatrix} 0 & n_{\perp T1}(3) \\ -r'_{\perp}(2)y' & r'_{\perp}(3) \end{vmatrix}}{detA}; \\ \overline{y_1} = y'; \\ \overline{z_1} = \dfrac{\begin{vmatrix} n_{\perp T1}(1) & 0 \\ r'_{\perp}(1)x & -r'_{\perp}(2)y' \end{vmatrix}}{detA}. \end{cases} \quad (21)$$

Here, *y'* has to be chosen in order to keep $\overline{z_1} > 0$ because the vector L_1 aligns in the positive *z'* direction (towards the receiver). A similar procedure can be used for the equation of L_2.

At last, the new acceptance angles are:

$$\beta^{+}_{3D} = \cos^{-1}\left(\frac{(\overline{x_1},\overline{y_1},\overline{z_1})\cdot \boldsymbol{r'}}{|(\overline{x_1},\overline{y_1},\overline{z_1})|\cdot|\boldsymbol{r'}|}\right); \quad (22)$$

$$\beta^{-}_{3D} = \cos^{-1}\left(\frac{(\overline{x_2},\overline{y_2},\overline{z_2})\cdot \boldsymbol{r'}}{|(\overline{x_2},\overline{y_2},\overline{z_2})|\cdot|\boldsymbol{r'}|}\right). \quad (23)$$

4. CODE EXTENSION AND VALIDATION

The above algorithm has been implemented in the existing suite of FirstOPTIC code in MATLAB. FirstOPTIC can now calculate the intercept factor of a trough collector under varying incidence angles; the slope errors may be specified with respect to both transversal and longitudinal planes as direct laboratory measurements. It is optional to take into account the end losses and spacing between collector elements.

To validate the developed code and test its capability, a series of optical error scenarios shown in TABLE 1 were created for a LS2 trough collector geometry (focal length $f = 1.49\ m$, aperture width $w = 5.0\ m$, receiver diameter $d = 0.07\ m$, collector length $l = 7.9\ m$). For simplicity, zero mean values were assumed for all errors given by a probability distribution and tracking error is neglected. The sun shape is assumed to be either a simple point source, a Gaussian distribution, or a CSR10 measurement by Neumann et al. [5].

TABLE 1: TEST CASES USING THE LS2 TROUGH COLLECTOR

Optics / Scenario	Sun Shape	Mirror Specularity	Slope Error	Receiver Position Error	Incidence Angle	End Losses
I	*Gaussian: σ = 2.5 mrad*	*Gaussian: σ = 6 mrad*	*None*	*None*	*30°*	*Yes*
II	*Point source*	*None*	$\varepsilon_x = 0$ $\varepsilon_y = 20\ mrad$	*None*	*60°*	*No*
III	*Point source*	*None*	*None*	*dx = 40 mm; dz = 50 mm.*	*60°*	*No*
IV	*Gaussian: σ = 2.5 mrad*	*Gaussian: σ = 6 mrad*	$\varepsilon_x = 6.8\ mrad$ $\varepsilon_y = 4\ mrad$	*dx = 20 mm; dz = 30 mm.*	*30°*	*No*
V	*CSR10*	*Gaussian: σ = 6 mrad*	*Data set: $\sigma(\varepsilon_x) = \sigma(\varepsilon_y)$ = 5.5 mrad*	*dx = 20 mm; dz = 30 mm.*	*60°*	*No*

For comparison, SolTrace [6], a Monte-Carlo ray-tracing tool originally developed for solar applications by NREL, is used to perform ray-tracing simulations for all test cases. For cases II and III, numerical results can also be readily derived from basic geometrical considerations: when the sun is assumed to be a point emitting source, the intercept factor can be determined directly by comparing the angular deviation of the reflected ray due to slope error with the acceptance angle limits of the receiver. Fig. 4 exhibits this simple procedure for case II, in which only longitudinal slope error is present. The angular deviation for reflected sun rays is plotted as a function of *x* along the collector aperture; the acceptance angle window is plotted as well. By comparing the two sets of angular data, a reflected sun ray will be intercepted by the receiver if its angular deviation falls into the acceptance angle window; it would miss the receiver otherwise. The collector intercept factor can then be readily calculated by integrating over the aperture. A similar procedure can be applied to case III.

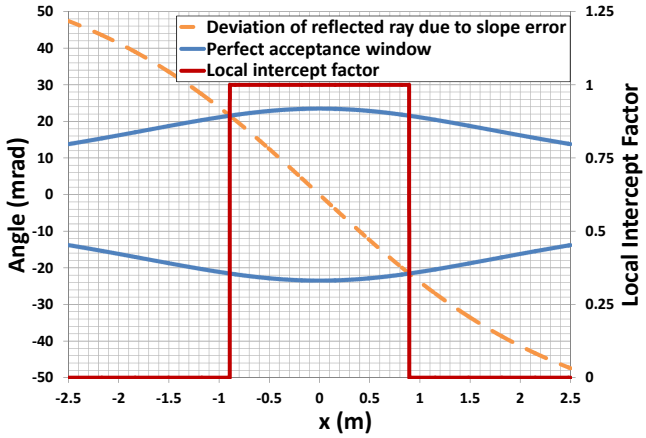

Fig. 4: Theoretical derivation of the local intercept factor for scenario II.

In TABLE 2, the intercept factors for the various cases listed in TABLE 1 are summarized for FirstOPTIC, the SolTrace (1 million sun rays were used for each case), and the numerical approach when possible. The results show excellent agreement between the three different approaches and validate the FirstOPTIC for non-zero incidence angles.

TABLE 2: INTERCEPT FACTOR FOR DIFFERENT METHODS

Method / Scenario	FirstOPTIC	SolTrace	Numerical
I	0.8541	0.8574	-
II	0.3574	0.3572	0.3573
III	0.4026	0.4026	0.4020
IV	0.7370	0.7403	-
V	0.5795	0.5816	-

5. CONCLUSIONS

FirstOPTIC [3] has been successfully extended to account for the 3-D effects of parabolic trough collectors and calculate the intercept factor for non-zero incidence angles. The new approach has been carefully benchmarked against ray-tracing results and numerical solutions (if available) with excellent agreement.

The analytical nature of the developed method allows fast evaluation of trough collector optical performance under varying incidence angles. In the future, FirstOPTIC is expected to conduct analysis on the 3-D effects of trough collectors, which would lead to a deep understanding of the optical performance of a trough collector under varying incidence angles and facilitate new collector designs and associated optical analysis.

6. ACKNOWLEDGEMENTS

The authors wish to thank the National Renewable Energy Laboratory (NREL) in the U.S. and the Department of Energy at the Politecnico di Milano University in Italy for supporting this work. The work at NREL was supported by the U.S. Department of Energy under Contract No. DE-AC36-08-GO28308. Special thanks to Allan Lewandowski and Tim Wendelin at NREL for their technical support on SolTrace. The authors also highly appreciate support from Dr. Ennio Macchi and Dr. Paolo Silva at Politecnico di Milano.

7. REFERENCES

(1) "Renewable 2011 Global Status Report," REN21, Paris, France, 2011 (2) A. Rabl, *Active Solar Collectors and Their Applications*. New York: Oxford University Press, 1985 (3) G. Zhu and A. Lewandowski, "A New Optical Evaluation Approach for Parabolic Trough Collectors: First-principle OPTical Intercept Calculation (FirstOPTIC)," *Submitted to the ASME Journal of Solar Energy Engineering,* 2011 (4) T. Wendelin, K. May, and R. Gee, "Video Scanning Hartmann Optical Testing of State-of-the-Art Parabolic Trough Concentrators," presented at the Solar 2006 Conference, Denver, Colorado USA, 2006 (5) A. Neumann, A. Witzke, S. A. Jones, and G. Schmitt, "Representative Terrestrial Solar Brightness Profiles," *Journal of Solar Energy Engineering,* vol. 124, pp. 198-204, 2002 (6) T. Wendelin, "SolTrace: A New Optical Modeling Tool for Concentrating Solar Optics," presented at the 2003 International Solar Energy Conference, Hawaii, USA, 2003.